PNAS
www.pnas.org

Supplementary Information for

Enhanced Ca^{2+} signaling, mild primary aldosteronism and hypertension in a mouse model of familial hyperaldosteronism (*Cacna1h*$^{M1560V/+}$)

Eric Seidel, Julia Schewe, Junhui Zhang, Hoang An Dinh, Sofia Forslund, Lajos Marko, Jörg Peters, Dominik N. Muller, Richard P. Lifton, Timothy Nottoli, Gabriel Stölting, Ute I. Scholl

Corresponding authors:

Ute Scholl, Email: ute.scholl@charite.de or Richard P. Lifton, Email: rickl@mail.rockefeller.edu

This PDF file includes:

Supplementary Methods

Figures S1 to S11

Table S1

Legends for Movies S1 to S2

Other supplementary materials for this manuscript include the following:

Movies S1 to S2

Supplementary Methods

Generation of the *Cacna1h*$^{M1560V/+}$ mouse model.

Potential Cas9 target guide (protospacer) sequences in proximity to *Cacna1h* M1560 were screened using the tool CRISPOR http://crispor.tefor.net/crispor.py. Several potential sequences were selected, sgRNAs were transcribed and tested for activity by microinjection with Cas9 into zygotes followed by culture to blastocyst. Activity was scored by the fraction of blastocysts with indels to the number of blastocysts genotyped.
The protospacer sequence CCTGGTGCTGCCGGCACTTG (reverse strand) was chosen due to its performance in the activity assay, despite the location of its Cas9 cleavage site 34 bases away from the desired A to G base change. A repair template oligonucleotide (ssODN) was synthesized by Integrated DNA Technologies to contain the specified A->G and 3 silent mutations designed to prevent Cas9 re-cleavage of the newly created allele (see sequences below). Components were mixed in injection buffer at a concentration of 30 ng/µl Cas9 (New England Biolabs), 15 ng/µl sgRNA, and 10 ng/µl ssODN, centrifuged, and microinjected into pronuclei of C57BL/6J zygotes. Embryos were transferred to the oviducts of pseudopregnant CD-1 foster females using standard techniques (1). The resulting pups were genotyped by Sanger sequencing (forward primer: 5'-ATCCTGTTGCGACAAGGCAC-3'; reverse primer: 5'-TTGGGATTGGAGCAAGTCGC-3'). Forty-five pups were genotyped, 6 of which contained the desired *Cacna1h*$^{M1560V/+}$ mutation (13%). Thirty-two mice contained heterozygous indel mutations (71%). Among these overlapping groups, four mice showed *Cacna1h*$^{M1560V/+}$ and an additional indel (9%). Back-crossing 4 mutant mice (3 with additional indels) to the C57BL/6J strain yielded a total of 47 pups (9 litters). Seventeen (36%) of these mice carried the desired *Cacna1h*$^{M1560V/+}$ mutation, five of which (2 males, 3 females) served as founder mice of the *Cacna1h*$^{M1560V/+}$ mouse strain. Further, 10 of the 47 pups (21%) contained an 8 bp indel (p.His1570Glnfs*83). Five mice (2 males, 3 females) carrying the p.His1570Glnfs*83 mutation served as founders of the *Cacna1h*$^{-/-}$ strain. Founders were backcrossed to C57BL/6J, and mutations in the three highest ranked potential exonic off-target sites (according to the CRISPOR tool, see above) were excluded by Sanger sequencing in the resulting pups used for further breeding (off-target 1 (*Cacna1g):* forward primer: 5'-CAGGAGCACTTCTCCCAGC-3'; reverse primer: 5'-GATCCCCGGGGCTGTTTAAT-3'; off-target 2 (*Emc3*): forward primer: 5'-CTCTGAGTCAGGTTAGAACTCAAG-3'; reverse primer: 5'- TGTACAGTAAACCTGACGGCT-3'; off-target 3 (*P2rx1*): forward primer: 5'- CTTATGCTTCTGATCCCACCCC-3'; reverse primer: 5'-GAATCTTGTGGTAGAGGCATTTC-3').

Cacna1h^{M1560V} sgRNA template primer (sgRNA underscored):
5'-
TGTAATACGACTCACTATAGGCCTGGTGCTGCCGGCACTTGGTTTTAGAGCTAGAAATAGC-3'

Repair template sequence (forward strand; intended mutations bold, sgRNA binding site underscored, target codon *italic*):
5'-
GGATGCTGCTCTACTTCATCTCCTTCCTGCTCATCGTCAGCTTCTTCGTGCTCAAC***G****T**G*TTTG
TGGGCGTGGTGGTGGAGAACTT**T**CA**T**AA**A**TGCCGGCAGCACCAGGAGGCGGAGGAAGCGC
GGCG-3'

Adrenal expression of the respective mutations in the *Cacna1h*$^{M1560V/+}$ and *Cacna1h*$^{-/-}$ strain was confirmed by Sanger sequencing of cDNA (forward primer: 5'-AACCTGGGTCAGGCGCT-3'; reverse primer: 5'-CAAAGTTGGTGAAGGTGGCG-3').

Animals and sample collection.

Briefly, mice were anaesthetized via i.p. injection of ketamine (100 mg/kg) and xylazine (10 mg/kg). For collection of blood or tissue for gene expression studies, blood was collected by cardiac puncture in Vacutainer tubes (EDTA, Becton Dickinson), centrifuged (10 min, 2000 g, 4 °C), and the supernatant (plasma) was stored at -20 °C until further use. Adrenal glands and kidneys were

harvested, and adrenal weight was measured. All organs were stored in RNAlater RNA stabilization reagent (Qiagen; 4 °C overnight, then -20 °C) until further use. For histology, organs of anaesthetized animals were fixed by transcardial perfusion using 10 ml PBS containing 10 U/ml heparin, followed by 10 ml 4% paraformaldehyde in PBS (pH 7.4; Santa Cruz). Adrenal glands, hearts and kidneys were harvested and subsequently fixed in 10% formalin solution (neutral buffered; Sigma Aldrich) for 18-24 h at 4 °C. After dehydrating in ethanol (70%, 80%, 96% and 100%) and xylene, samples were embedded into paraffin (Merck Millipore) and stored at room temperature until further use.
Spot urine was collected on three consecutive days in the morning. After 1 week of recovery, blood was collected under anaesthesia via cardiac puncture (26G needle, 1 ml syringe) into Microtainer (Lithium-Heparin) tubes (Becton Dickinson). Blood was centrifuged immediately (4 °C, 2000 g, 10 min), and blood and urine were stored at 4°C for up to 7 days.
NSD contained 0.24% sodium. HSD consisted of E15431–34 (containing 1.71% sodium, Ssniff Spezialdiäten) and 1% NaCl via drinking water for 4 weeks followed by collection of blood and tissue as described above. Wildtype controls were littermates of knockin animals, with the exception of aged mice (Fig. S2 and S6). In those cases, age-matched C57BL/6J wildtype animals were ordered from Charles River Laboratories.

H&E and Sirius red staining.
Briefly, embedded tissue was cut into 5 µm sections, deparaffinized with xylene and rehydrated in ethanol (100%, 95%, 90%, 80%, and 70%) and deionized water. For H&E staining, rehydrated sections were subsequently incubated in hematoxylin (Sigma Aldrich) for 3 min, rinsed with tap water, dipped in acid ethanol (0.25% HCl in 70% ethanol), incubated in eosin (Carl Roth) for 30 s, dehydrated in 100% ethanol and xylene and mounted using VectaMount (Vector Labs). For Sirius red staining, sections were incubated in hematoxylin for 8 min, washed in tap water, incubated in 0.25 g/L Direct Red 80 (Sigma Aldrich) in 1.3% picric acid (Sigma Aldrich) for 60 min, washed in 0.5% acetic acid, dehydrated (70%, 95% and 100% ethanol and xylene) and mounted using VectaMount.

***In situ* hybridization.**
In images comprising the entire adrenal gland, the number of *Cyp11b2* positive cells was quantified relative to the total cell number using Fiji according to the manufacturer's recommendations. Adrenal images were cropped around the capsule, and trainable Weka Segmentation plugin was used to create pixel-based segmentations using three areas of probe signal, counterstain and background as classifiers and Mean, Maximum, Variance, Minimum and Entropy as training features. In segmentations, threshold was adjusted to probe signal using Otsu's method, overlapping cells were separated using the watershed function and particles were counted using "0-infinity" as size parameter and "0.0-1.0" as circularity parameter. Afterwards, false positives were assessed manually. For determination of total cell number, adrenal images were cropped around the capsule, and the "color deconvolution from ROI" function of Fiji was used choosing probe signal, counterstain and background as ROIs (Regions of interest). In counterstain images, threshold was adjusted to probe signal using Otsu's method, and particles were counted using "0-infinity" as size parameter and "0.0-1.0" as circularity parameter. For additional determination of average staining intensity, RawIntDen values were measured in the same segmentations used above (limiting measurements to probe threshold) and normalized to the number of positive cells. Data were analyzed using a linear mixed model (2) (for fraction of positive cells) or a generalized linear mixed model (for staining intensity; data were not normally distributed).

Determination of PRC.
Briefly, high binding RIA tubes (Greiner Bio-One) were coated with anti-AT-I antibodies and subsequently blocked with 0.5% BSA.
Pre-treated samples and 125I-labeled AT-I (activity of 5000 cpm; Amersham Biosciences) were then incubated for 20 h at room temperature, washed three times with washing buffer, and the AT-I concentration was measured using a γ-counter (Berthold LD 2111). The concentration was determined according to a standard curve.

Blood pressure measurements.
Briefly, a telemetric catheter (DSI PhysioTel PA-C10; weight 1.4 g; Data Science International) was implanted in 3-month-old male mice under general anesthesia using i.p. ketamine 100 mg/kg + xylazine 10 mg/kg. The right common carotid artery was dissected, the blood flow of the common carotid artery was stopped caudally using a miniature clamp, and the catheter was placed into the vessel. The wound was closed using 3–0 Prolene, and mice received Rimadyl 5 mg/kg s.c. intraoperatively followed by Metamizol 1350mg/kg/day via drinking water for three days. Mice were fed a standard diet (E15430-047 containing 0.24% sodium, ssniff Spezialdiäten). After 1 week of recovery, blood pressure and heart rate were recorded for 20 days (every 5 min, each 10 s). Afterwards, mice were fed a HSD (see above) for 28 days. Fig. 6 represents data between days 13 and 20 post surgery on NSD and between days 39 and 47 (after 2 weeks HSD). Locomotor activity was recorded based on signal strength changes in the orientation and distance of the animal relative to the receiver. Quality controlled sensor data were analyzed by mixed effect modeling (treating animal ID and timepoint as random effects, genotype and day/night state as fixed effects, disabling REML estimation) using the lme4 (2) R package, the lmtest (3) R package and the ggplot2 (4) R package, assessing significance by likelihood ratio.

Calcium imaging.
Successive frames from each channel were divided to yield a video of the 340/385 nm ratio with 5 frames per second. Individual cells were selected manually by their activity at a perfusion with 1 nmol/l Ang II. Mean ratio traces were taken for each cell. Identification of spikes as well as mean, baseline and peak ratio determination was performed using a custom written python script (5).
For calibration of 340/385 nm ratios to calcium concentrations, slices stained with Fura-2 AM were incubated with solutions of known extracellular calcium concentrations (Calcium Calibration Buffer Kit, Promocell) supplemented with 25 µmol/l ionomycin. Solutions were chosen to yield final free calcium concentrations between 0 and 39.8 µmol/l. 340/385 nm ratios were observed over time. Final values were determined once recordings remained within 5% of each other for either a) more than 30 minutes or b) for at least two observations (≥15 minutes) after a change in ratio values. Final ratio values were plotted against the calcium concentrations and fitted to a Hill equation to determine the Kd of Fura-2 in Zona glomerulosa cells. Ratios from other recordings could then be converted into $[Ca^{2+}]$ according to Grynkiewicz et al. (6). Statistical analysis was performed using mixed effect modelling in R using the lme4 package (2). Individual animals were treated as random and their genotype as fixed effect. Significance of parameters was determined by likelihood ratio comparisons using χ^2 statistics with a degree-of-freedom of 2, and P-values were calculated. Inclusion of further effects generally did not significantly improve the variance explained by those models. Recordings were loaded into Fiji (http://fiji.sc), and 340 and 385 nm channels were separated.

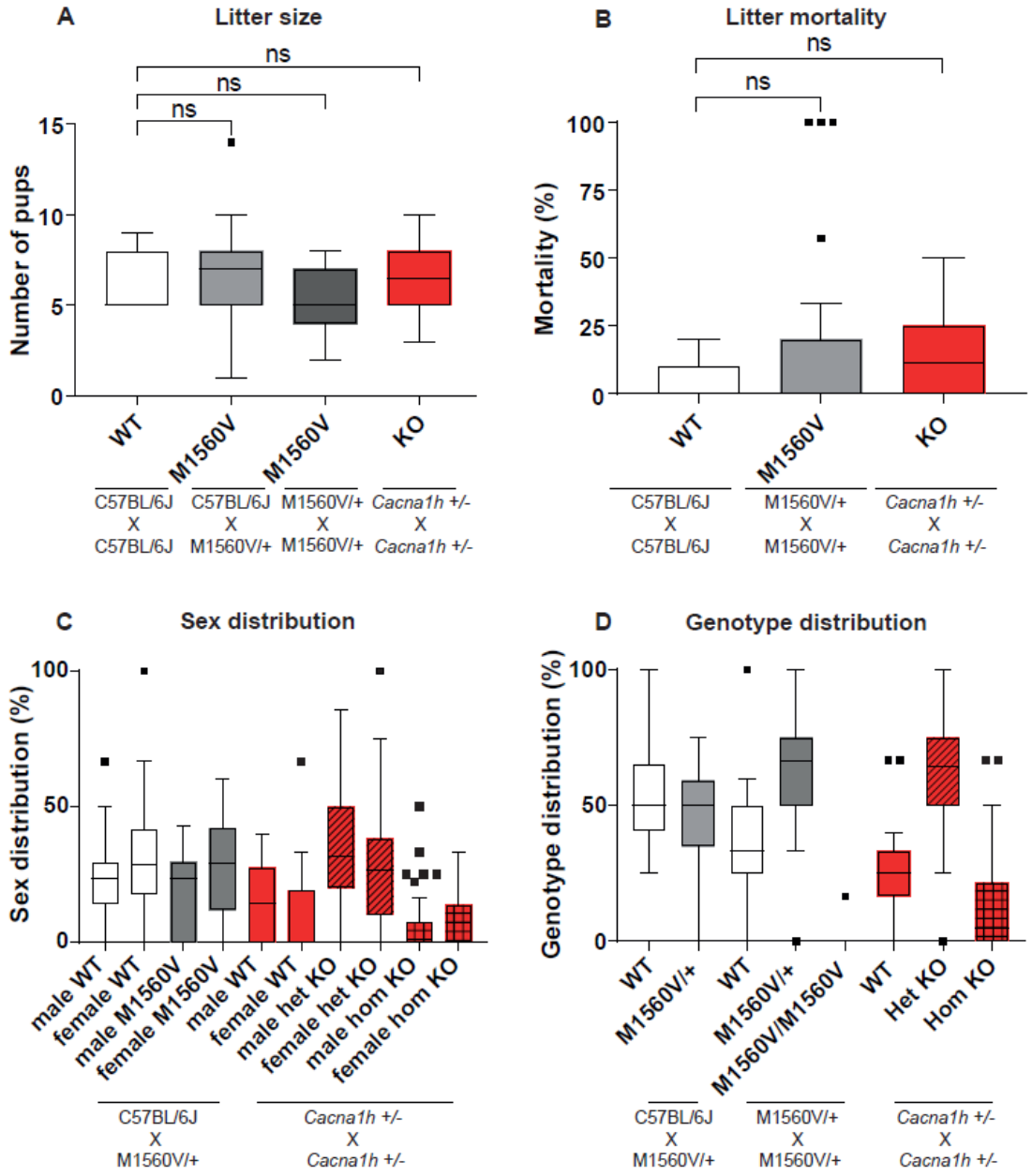

Fig. S1. Litter size, mortality rate, sex and genotype distribution in *Cacna1h*$^{M1560V/+}$ and *Cacna1h*$^{-/-}$ mice. (*A*) Litter size is unchanged in *Cacna1h*$^{M1560V/+}$ (C57BL/6J X *Cacna1h*$^{M1560V/+}$ and *Cacna1h*$^{M1560V/+}$ X *Cacna1h*$^{M1560V/+}$ breedings) and *Cacna1h*$^{-/-}$ (*Cacna1h*$^{+/-}$ X *Cacna1h*$^{+/-}$ breeding) compared to WT (C57BL/6J X C57BL/6J). WT: N = 5 litters; *Cacna1h*$^{M1560V/+}$ (C57BL/6J X *Cacna1h*$^{M1560V/+}$): N = 25 litters; P > 0.9999; *Cacna1h*$^{M1560V/+}$ (*Cacna1h*$^{M1560V/+}$ X *Cacna1h*$^{M1560V/+}$): N = 27 litters; P > 0.9999; *Cacna1h*$^{-/-}$: N = 32 litters; P > 0.9999; Kruskal–Wallis test, Dunn's MCP. (*B*) Litter mortality is not significantly changed in *Cacna1h*$^{M1560V/+}$ (*Cacna1h*$^{M1560V/+}$ X *Cacna1h*$^{M1560V/+}$ breeding) and *Cacna1h*$^{-/-}$ (*Cacna1h*$^{+/-}$ X *Cacna1h*$^{+/-}$ breeding) strain (WT: N = 5; *Cacna1h*$^{M1560V/+}$: N = 27; > 0.9999; *Cacna1h*$^{-/-}$: N = 32; P = 0.3825; Kruskal–Wallis test, Dunn's MCP). (*C*) Sex distribution is unchanged in *Cacna1h*$^{M1560V/+}$ (C57BL/6J X *Cacna1h*$^{M1560V/+}$ breeding; in total 160 weaned pups from 24 litters) and *Cacna1h*$^{-/-}$ (*Cacna1h*$^{+/-}$ X *Cacna1h*$^{+/-}$ breeding, 180 weaned pups from 32 litters) (male WT: N = 37, expected: 43; male *Cacna1h*$^{M1560V/+}$ N = 31,

expected 37; female WT: N = 49, expected: 43; female *Cacna1h*$^{M1560V/+}$: N = 43, expected: 37; P = 0.2354 for male vs. female WT and P = 0.2007 for male vs. female *Cacna1h*$^{M1560V/+}$; two-tailed binomial test; male WT: N = 28, expected: 24; male *Cacna1h*$^{+/-}$: N = 59, expected: 53.5; male *Cacna1h*$^{-/-}$: N = 11, expected: 12.5; female WT: N = 20, expected: 24; female *Cacna1h*$^{+/-}$: N = 48, expected: 53.5; female *Cacna1h*$^{-/-}$: N = 14, expected: 12.5; P = 0.3718 for male vs. female WT; P = 0.3776 for male vs. female *Cacna1h*$^{+/-}$ and P = 0.6900 for male vs. female *Cacna1h*$^{-/-}$; two-tailed binomial test). Shown is the percentage of the indicated sex and genotype in relation to the number of weaned pups per litter. (*D*) Genotype distribution in *Cacna1h*$^{M1560V/+}$ and *Cacna1h*$^{-/-}$ strains. In C57BL/6J X *Cacna1h*$^{M1560V/+}$ breedings (in total 160 weaned pups from 24 litters), genotypes are not differentially distributed (WT: N = 86, expected: 80; *Cacna1h*$^{M1560V/+}$: N = 74, expected: 80; P = 0.4248; two-tailed binomial test). In *Cacna1h*$^{M1560V/+}$ X *Cacna1h*$^{M1560V/+}$ breedings (117 weaned pups from 24 litters), only one *Cacna1h*$^{M1560V/M1560V}$ mouse survived until weaning (WT: N = 40, expected: 29.25; *Cacna1h*$^{M1560V/+}$: N = 76, expected: 58.5 and *Cacna1h*$^{M1560V/M1560V}$: N = 1, expected: 29.25; P < 0,0001; Chi-square test, DF = 2). In *Cacna1h*$^{+/-}$ X *Cacna1h*$^{+/-}$ breedings (180 weaned pups from 32 litters), fewer *Cacna1h*$^{-/-}$ pups than expected were born (WT, N = 48, expected: 45; *Cacna1h*$^{+/-}$: N = 107, expected: 90 and *Cacna1h*$^{-/-}$: N = 25, expected: 45; P = 0.0021; Chi-square test, DF = 2). Shown is the percentage of the indicated genotype in relation to the number of weaned pups per litter. ns, p > 0.05. All data are shown in box plots (box, interquartile range; whiskers, 1.5 times the interquartile range; line, median; dots, outliers).

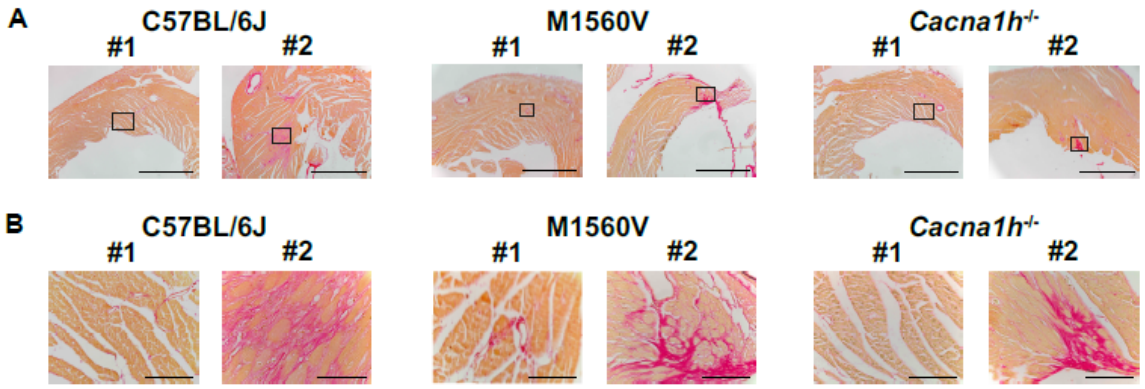

Fig. S2. Cardiac Sirius red stainings in aged WT, *Cacna1h*$^{M1560V/+}$ and *Cacna1h*$^{-/-}$ (KO) mice. *Cacna1h* $^{-/-}$ mice show localized areas of cardiac fibrosis, but such areas are also identified in other genotypes. (A and B) Sirius red staining of transverse heart sections of 48-60 weeks old C57BL/6J, *Cacna1h*$^{M1560V/+}$ and *Cacna1h*$^{-/-}$ mice. Two of 5 animals per genotype (one male, one female each) are shown. Scale bars: (*A*), 1 mm; (*B*), 100 µm.

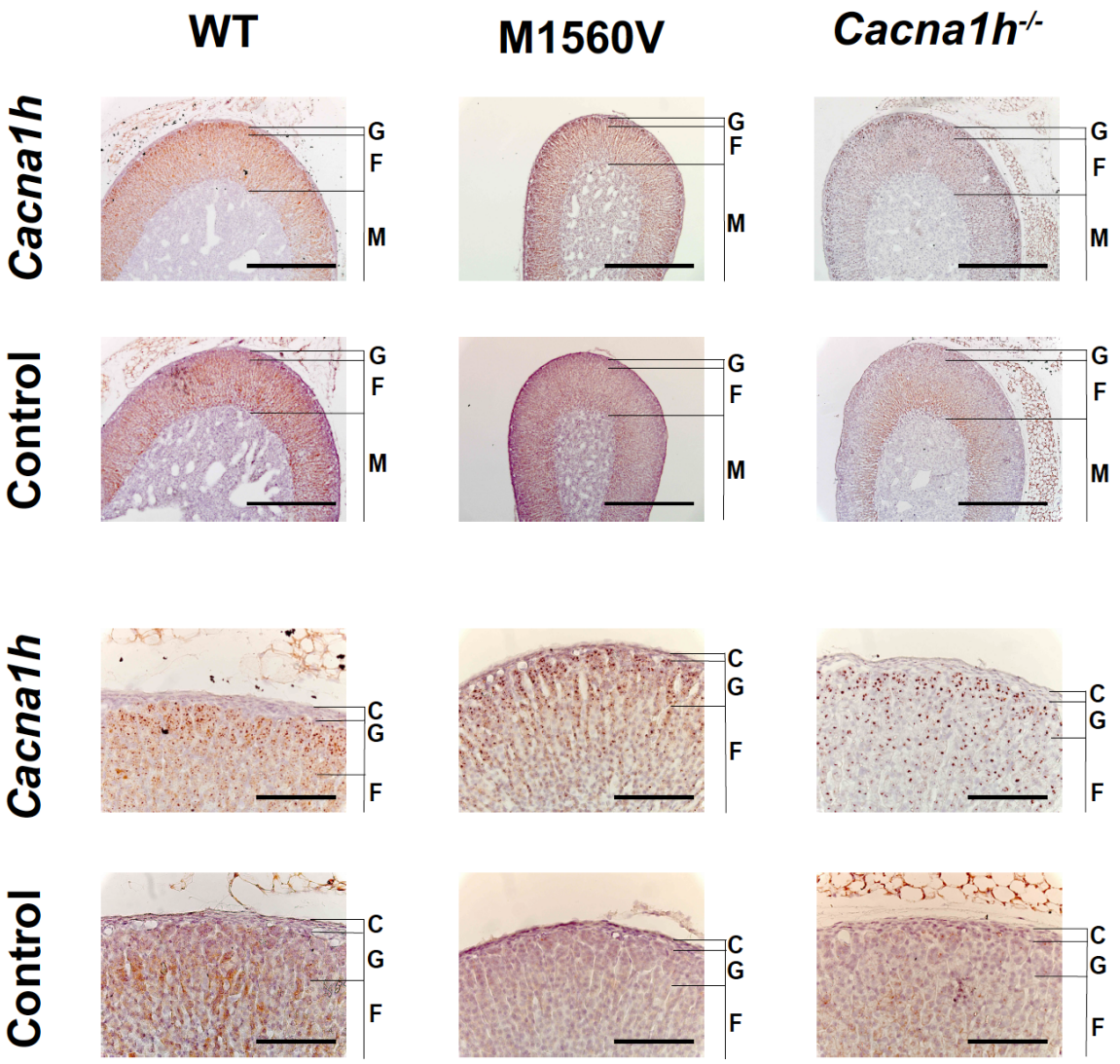

Fig. S3. Adrenal sections of WT, *Cacna1h*$^{M1560V/+}$ and *Cacna1h*$^{-/-}$ mice. *Cacna1h* is expressed in the zona glomerulosa and the zona fasciculata. *In situ* hybridization with corresponding negative controls (see *Materials and Methods*, one of 3-4 animals of each genotype is shown. C: capsule; G: glomerulosa; F: fasciculata; M: medulla. Scale bars: 500 µm (upper two rows); 100 µm (lower two rows).

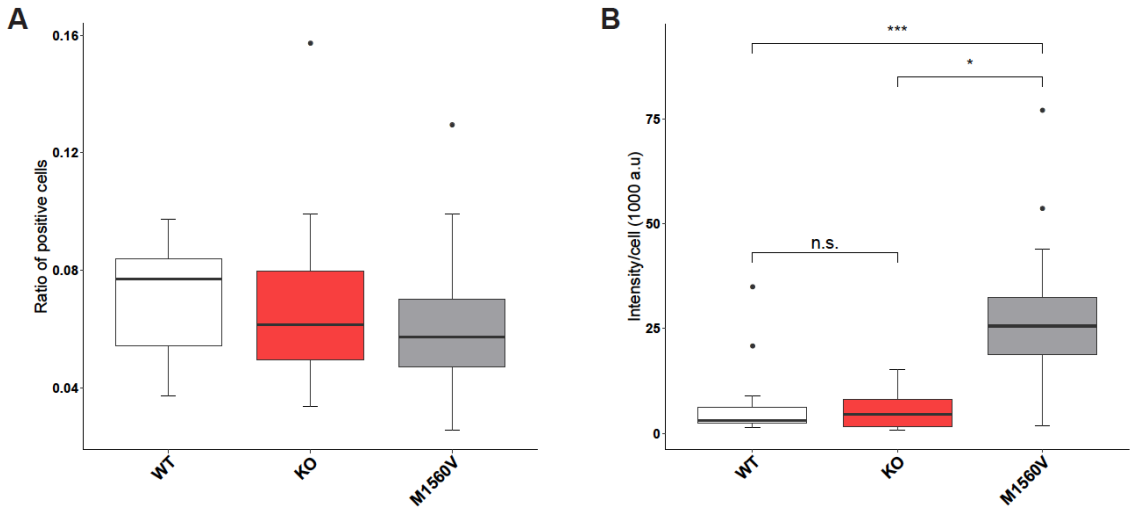

Fig. S4. Analysis of *in situ* hybridization. N = 3 animals per genotype. For each animal, three sections from each gland (right and left) were stained, with the exception of M1560V (one slide from one animal missing), and for KO (one slide each from two animals missing). All data are shown in box plots (box, interquartile range; whiskers, 1.5 times the interquartile range; line, median; dots, outliers). (*A*) Fraction of *Cyp11b2*-positive cells in whole adrenal sections (see *Materials and Methods*). There is no significant effect of genotype on the fraction of positive cells (linear mixed model, likelihood ratio comparison, p = 0.8725. (*B*) Staining intensity of positive area normalized by cell number. Staining intensity is higher for M1560V (generalized linear mixed model, LR comparison, p = 0.009447 for genotype; post-hoc estimated marginal means analysis with FDR adjusted p-values for a 3-way comparison: WT versus M1560V, p = 0.0002 (***), KO versus M1560V, p = 0.0215 (*), WT versus KO, p = 0.1181 (n.s.). a.u., arbitrary units.

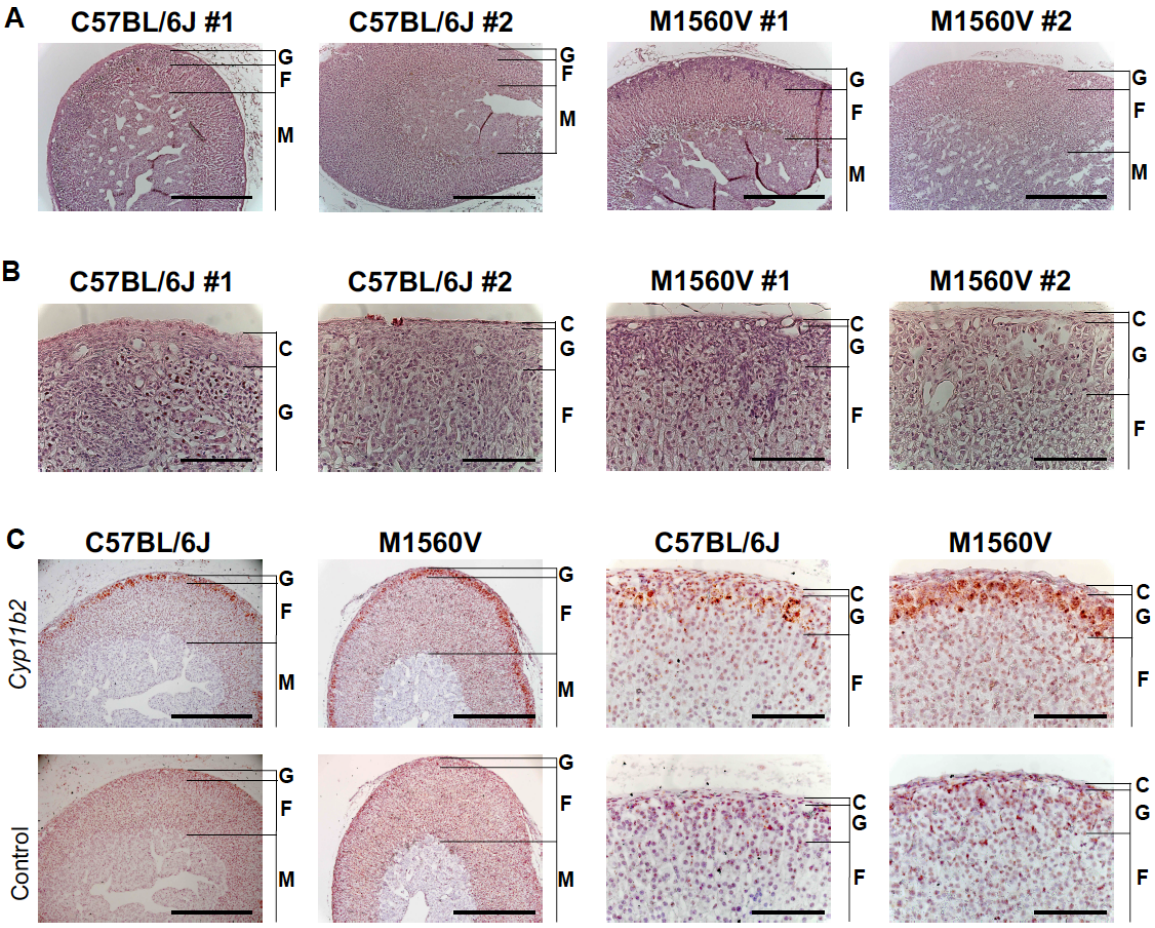

Fig. S5. Adrenal morphology and *Cyp11b2* expression in *Cacna1h*$^{M1560V/+}$ mice and controls (ages 48-60 weeks). (*A* and *B*) H&E staining (2 of 5-6 animals each are shown; C57BL/6J: 2 males, M1560V: 1 male and 1 female; C: capsule; G: glomerulosa; F: fasciculata; M: medulla). (*C*) *In situ* hybridization for *Cyp11b2* and corresponding negative controls (see *Materials and Methods*, one male animal of 3 animals each is shown; C: capsule; G: glomerulosa; F: fasciculata; M: medulla). Scale bars: (*A*, *C*, first two images from left), 500 µm; (*B, C*, third and fourth image from left), 100 µm.

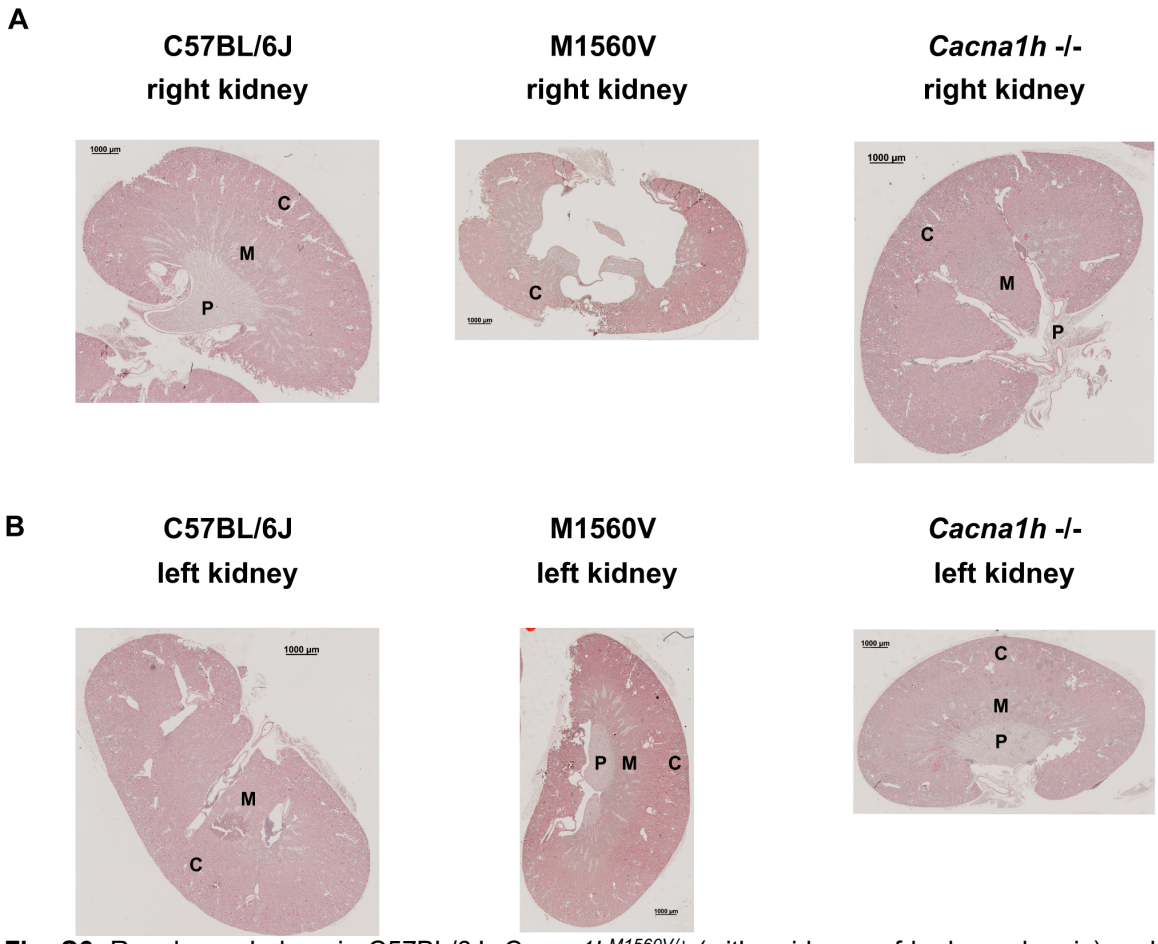

Fig. S6. Renal morphology in C57BL/6J, *Cacna1h*$^{M1560V/+}$ (with evidence of hydronephrosis) and *Cacna1h*$^{-/-}$ mice (ages 48-60 weeks). H&E stainings of (*A*) right and (*B*) left kidneys are shown (one male animal of 4-6 animals each). C, cortex; M, medulla; P, pyelon. Scale bar, 1000 µm.

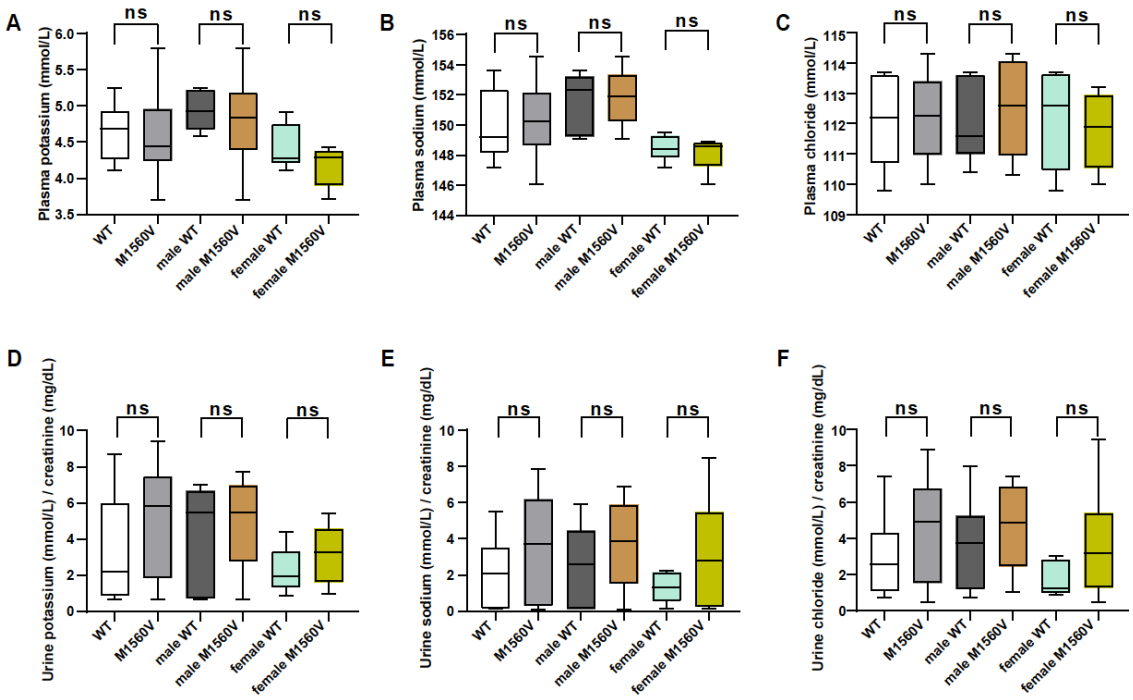

Fig. S7. Concentrations of plasma and urine electrolytes are unchanged in *Cacna1h*$^{M1560V/+}$ mice. Plasma levels of potassium (*A*) (WT: N = 11; *Cacna1h*$^{M1560V/+}$: N = 14; P = 0.6573; unpaired two-tailed t-test; male WT: N = 5; male *Cacna1h*$^{M1560V/+}$: N = 9; P = 0.7710; female WT: N = 6; female *Cacna1h*$^{M1560V/+}$: N = 5; P = 0.5919; one-way ANOVA including Sidak's MCP), sodium (*B*) (WT: N = 11; *Cacna1h*$^{M1560V/+}$: N = 14; P = 0.4875; unpaired two-tailed t-test; male WT: N = 5; male *Cacna1h*$^{M1560V/+}$: N = 9; P > 0.9999; female WT: N = 6; female *Cacna1h*$^{M1560V/+}$: N = 5; P > 0.9999; Kruskal-Wallis test including Dunn's MCP) and chloride (*C*) (WT: N = 11; *Cacna1h*$^{M1560V/+}$: N = 14; P = 0.9894; unpaired two-tailed t-test; male WT: N = 5; male *Cacna1h*$^{M1560V/+}$: N = 9; P = 0.9539; female WT: N = 6; female *Cacna1h*$^{M1560V/+}$: N = 5; P = 0.8925; one-way ANOVA including Sidak's MCP) do not differ between WT and *Cacna1h*$^{M1560V/+}$: mice. Creatinine-normalized urine levels of potassium (*D*) (WT: N = 11; *Cacna1h*$^{M1560V/+}$: N = 15; P = 0.2465; unpaired two-tailed t-test; male WT: N = 6; male *Cacna1h*$^{M1560V/+}$: N = 9; P = 0.8593; female WT: N = 5; female *Cacna1h*$^{M1560V/+}$: N = 6; P = 0.7608; one-way ANOVA including Sidak's MCP), sodium (*E*) (WT: N = 11; *Cacna1h*$^{M1560V/+}$: N = 15; P = 0.0604; unpaired two-tailed t-test; male WT: N = 6; male *Cacna1h*$^{M1560V/+}$: N = 9; P = 0.5863; female WT: N = 5; female *Cacna1h*$^{M1560V/+}$: N = 6; P = 0.3899; one-way ANOVA including Sidak's MCP) and chloride (*F*) (WT: N = 11; *Cacna1h*$^{M1560V/+}$: N = 15; P = 0.0872; unpaired two-tailed t-test; male WT: N = 6; male *Cacna1h*$^{M1560V/+}$: N = 9; P = 0.7514; female WT: N = 5; female *Cacna1h*$^{M1560V/+}$: N = 6; P = 0.3842; one-way ANOVA including Sidak's MCP) do not differ between WT and *Cacna1h*$^{M1560V/+}$: mice. All data are shown in box plots (box, interquartile range; whiskers, 1.5 times the interquartile range; line, median; dots, outliers); N values are animals. ns, p > 0.05. See Table 1 for corresponding mean values.

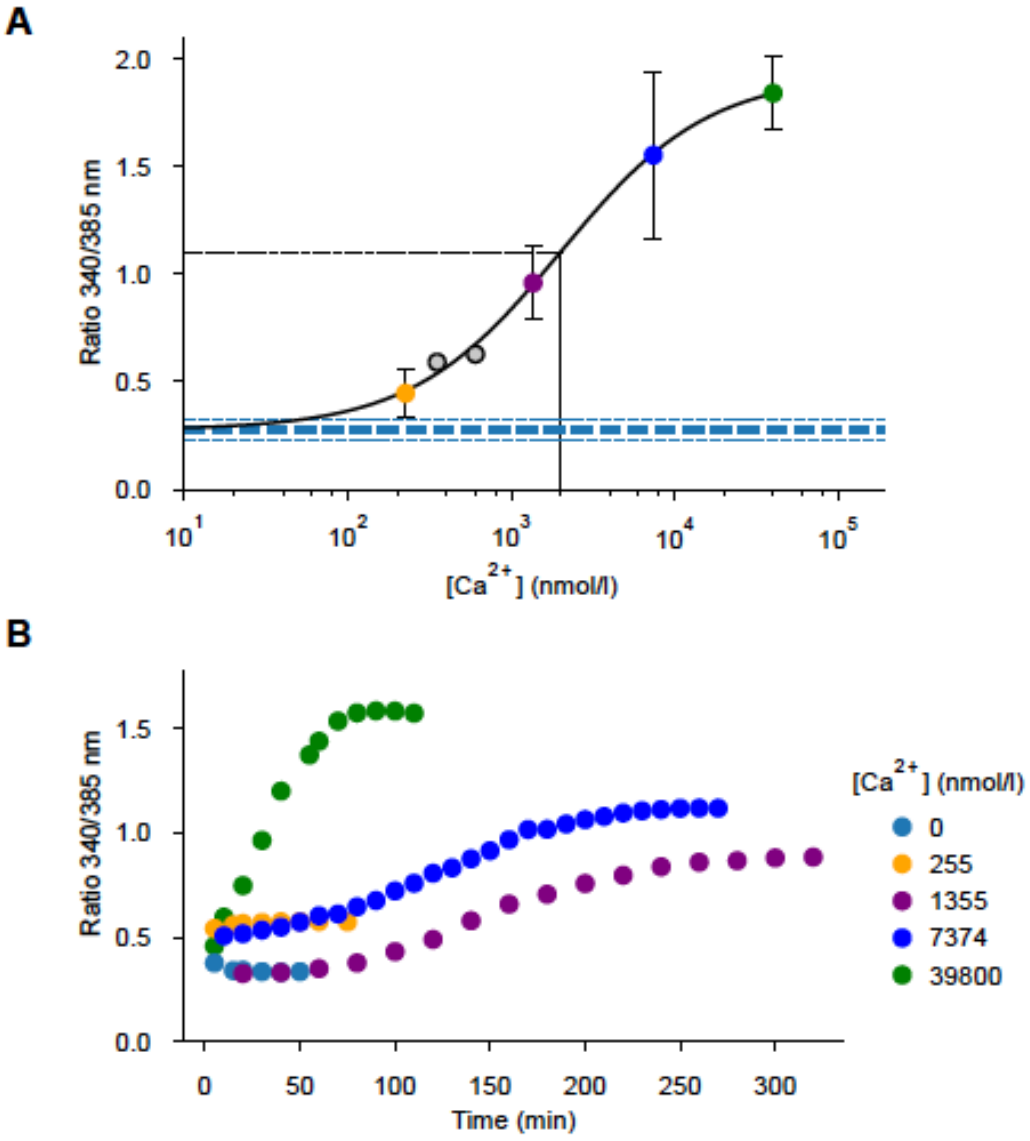

Fig. S8. Calibration of Fura-2 in zona glomerulosa cells reveals a high Kd. (***A***) Plot of the measured 340/385 nm ratios at fixed Ca^{2+} concentrations. Intracellular [Ca^{2+}] were clamped using ionomycin. The mean of the ratio in the absence of calcium is shown as a thick blue horizontal dashed line with the standard deviation as thinner lines above and below. Otherwise means are shown as circles ± SD for sample sizes larger than 1 (sample sizes at the indicated [Ca^{2+}] are: 0 nmol/l: 7; 225 nmol/l: 4; 351 nmol/l: 1; 602 nmol/l: 1; 1355 nmol/l: 5; 7374 nmol/l: 3; 39800 nmol/l: 7. Data were fit using the Hill equation to yield a Kd of approximately 2 µM (at the intersection of the dashed black lines). [Ca^{2+}] at 351 and 602 nmol/l are shown in gray. (***B***) Representative examples of the measured 340/385 nm ratios over time from the beginning of the incubation with ionomycin at various [Ca^{2+}]. Colors are the same as in *A*. Higher concentrations required longer incubations.

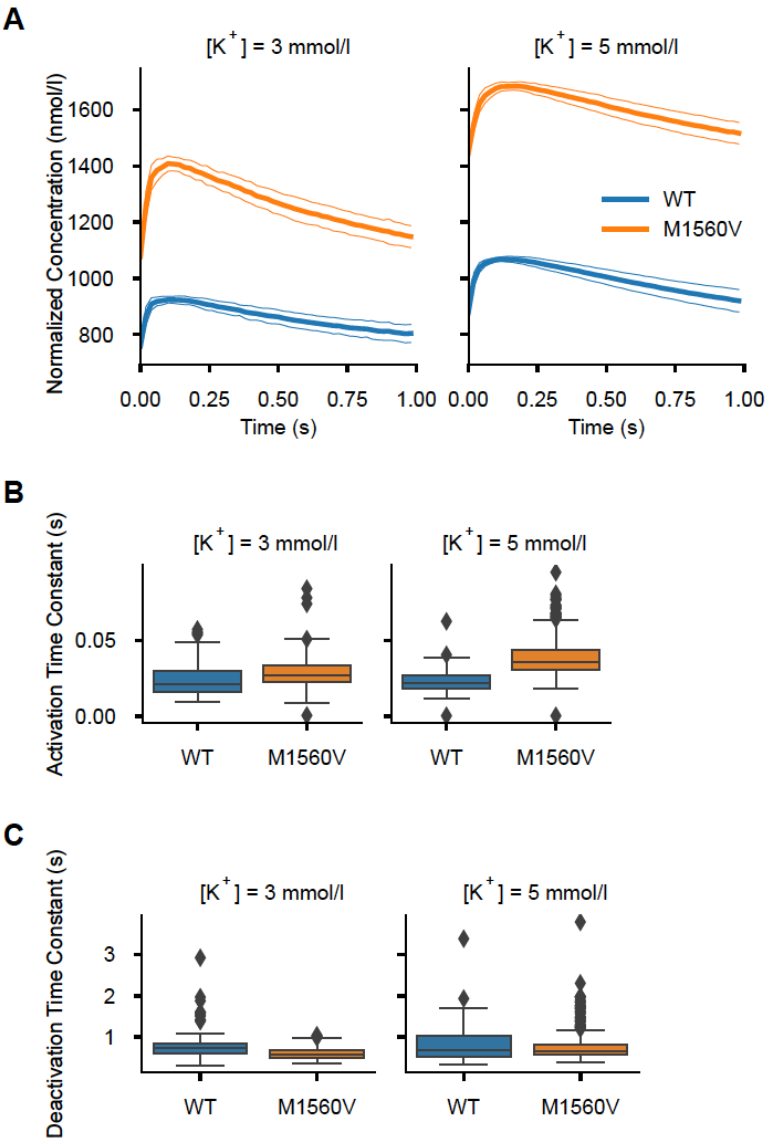

Fig. S9. Spike kinetics are unchanged between genotypes. (*A*) Average spikes were obtained at the indicated potassium concentrations at 1000 pM Ang II (thick lines). Cells were loaded with the non-ratiometric dye Calbryte 520 AM and recorded with a frame rate of 50 frames/s. Intensity values of all spikes were normalized to the baseline and peak values obtained by the calibrated Fura-2 AM recordings. The thin lines indicate the upper and lower value of the standard deviation. (*B*) The interval between the beginning and the peak of each spike was fit with an exponential function giving the time constant of the activation. Values are not statistically different as assessed by likelihood ratio test. (*C*) The interval between the peak and the end of each spike was fit with an exponential function giving the time constant of the deactivation. (3 mmol/l K^+: N (spikes WT/M1560V) = 104/126, P (activation) = 0.1235, P (deactivation) = 0.2373; 5 mmol/K^+: N = 141/323, P (activation) = 0.3705, P (deactivation) = 0.9008). Values were assessed by likelihood ratio test of linear

mixed models. Data in *B* and *C* are shown in box plots (box, interquartile range; whiskers, 1.5 times the interquartile range; line, median; dots, outliers).

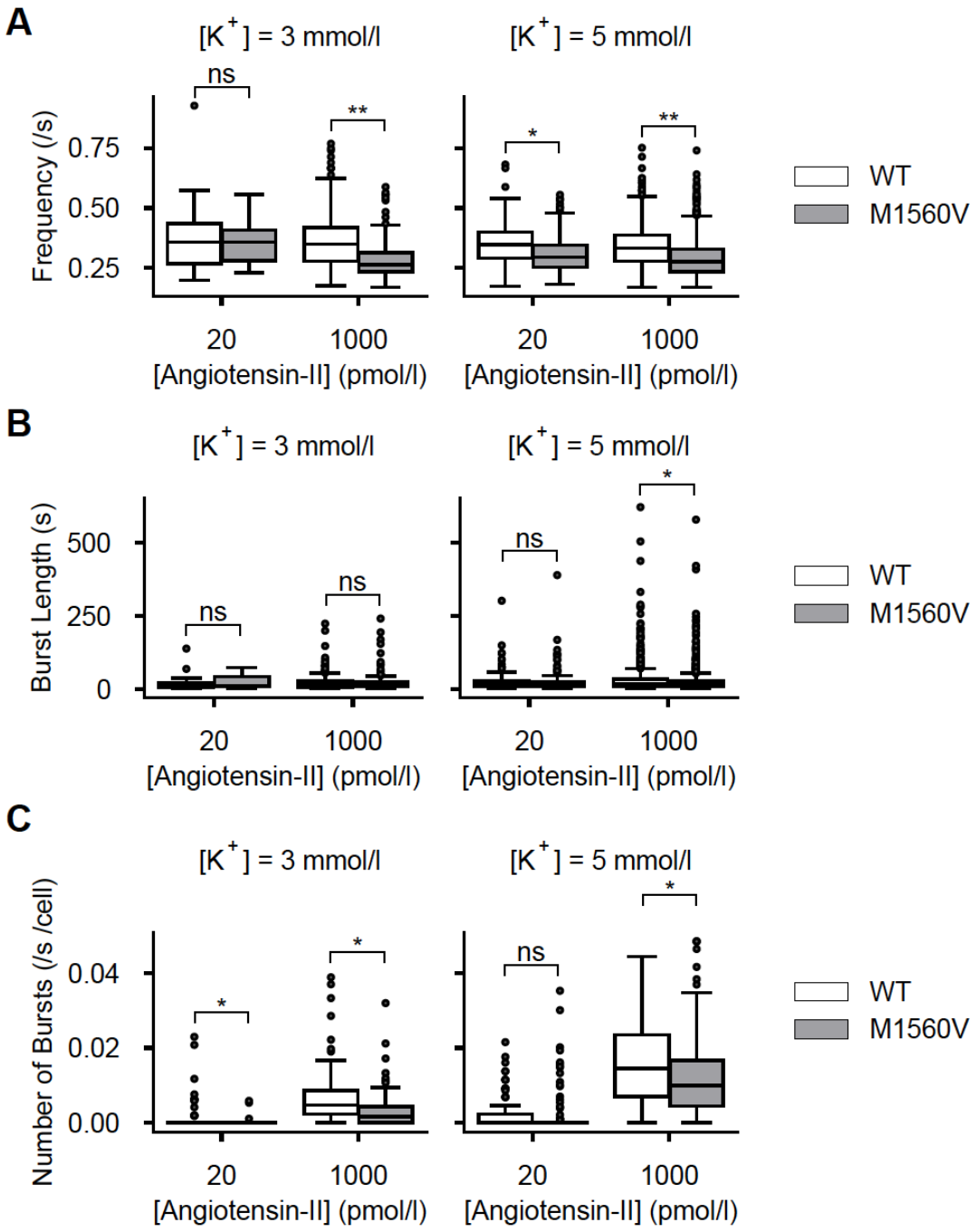

Fig. S10. Calcium bursting in adrenal slices from *Cacna1h*$^{M1560V/+}$ mice. (*A*) Average frequencies of calcium oscillations during bursts demonstrating a slower frequency in cells from *Cacna1h*$^{M1560V/+}$ slice preparations at high Ang II levels. For 3 mmol/l K^+: 20 pmol/l AT-II: N (bursts WT/M1560V) = 52/9, P = 0.8695; 1000 pmol/l AT-II: N = 295/165, P = 0.0026; for 5 mmol/l K^+: 20 pmol/l AT-II: N = 101/170, P = 0.0114; 1000 pmol/l AT-II: N = 756/773, P = 0.0013. (*B*) The average length of bursts is only affected at high concentrations of Ang II and potassium. For 3 mmol/l K^+: 20 pmol/l AT-II: N (bursts WT/M1560V) = 52/9, P = 0.2245; 1000 pmol/l AT-II: N = 295/165, P = 0.9562; for 5 mmol/l K^+: 20 pmol/l AT-II: N = 101/170, P = 0.3430; 1000 pmol/l AT-II: N = 756/773, P = 0.0428. (*C*) The number of bursts per condition and cell as normalized to time. Burst durations in cells from WT slice preparations are slightly longer for most conditions. For 3 mmol/l K^+: 20 pmol/l AT-II: N (cells

WT/M1560V) = 100/92, P = 0.0414; 1000 pmol/l AT-II: N = 100/99, P = 0.0152; for 5 mmol/l K^+: 20 pmol/l AT-II: N = 98/117, P = 0.8464; 1000 pmol/l AT-II: N = 98/128, P = 0.0334) P values were calculated using a likelihood ratio test of linear mixed models and are indicated as follows: ns, ≥ 0.05; *, <0.05; **, <0.01. Data are shown in box plots (box, interquartile range; whiskers, 1.5 times the interquartile range; line, median; dots, outliers).

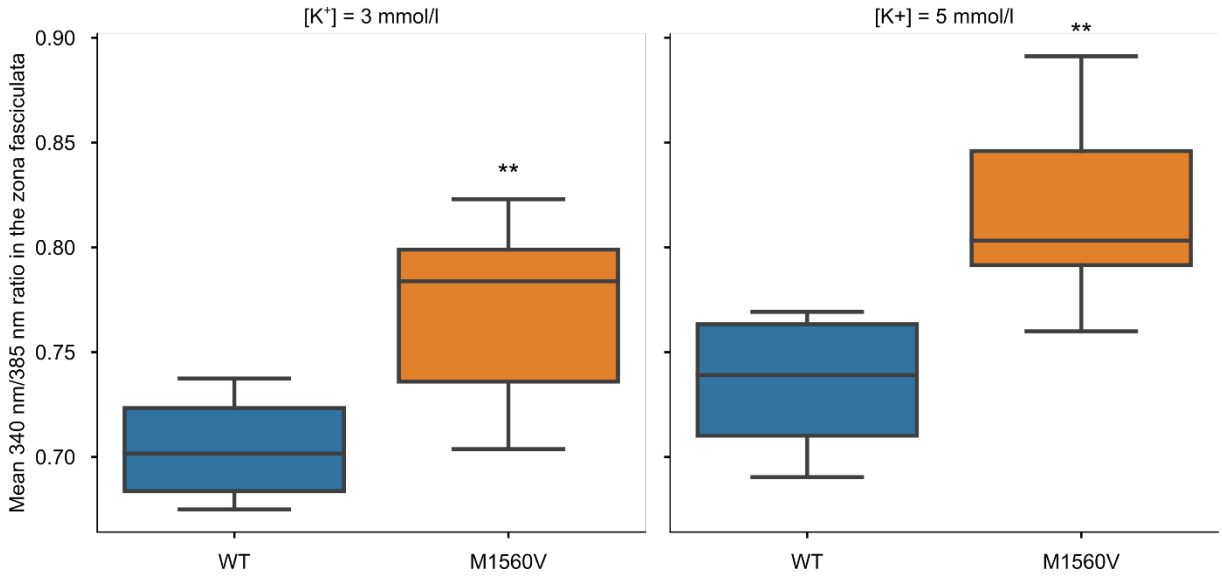

Fig. S11. Comparison of the mean 340/385 nm ratio in the zona fasciculata. Ratios, positively correlating with the intracellular calcium concentration, were obtained from four different cell columns within the zona fasciculata of each slice stained with Fura-2 AM. No difference was seen across varying Ang II concentrations, so recordings were only separated according to the potassium concentration of the external solution. At both [K^+], mean ratios were higher in *Cacna1h*$^{M1560V/+}$ slices indicating higher intracellular calcium concentrations in mice heterozygous for the M1560V mutation (Two-tailed Mann-Whitney U; 3 mmol/l [K^+]: N (WT/M1560V) = 7/9 slices, P = 0.003 (**); 5 mmol/l [K^+]: N = 4/9 slices, P = 0.008 (**)). Data are shown in box plots (box, interquartile range; whiskers, 1.5 times the interquartile range; line, median; dots, outliers).

Table S1. Results of calcium imaging.

Mean Calcium Concentration (Fig. 7):

K^+ (mM)	AT-II (pM)	WT mean (nM)	WT SD	WT (N)	Het mean (nM)	Het SD	Het (N)	P
3	0	767.8	262.0	125	936.5	181.3	139	0.0255 (*)
3	20	749.9	229.4	125	905.6	156.2	109	0.0058 (**)
3	1000	763.0	199.5	125	1098.2	291.0	124	< 0.0001 (***)
5	0	805.1	192.1	105	1219.6	266.2	125	0.0002 (***)
5	20	769.5	164.2	105	1163.2	269.9	125	0.0003 (***)
5	1000	921.2	231.1	105	1484.4	441.2	138	0.0015 (**)

Baseline Calcium Concentration (Fig. 7):

K^+ (mM)	AT-II (pM)	WT mean (nM)	WT SD	WT (N)	Het mean (nM)	Het SD	Het (N)	P
3	0	767.1	261.2	125	927.8	157.3	139	0.0260 (*)
3	20	748.1	229.1	125	904.7	156.0	109	0.0056 (**)
3	1000	739.1	203.9	125	1077.3	291.2	124	<0.0001 (***)
5	0	804.9	191.5	105	1216.5	269.3	125	0.0003 (***)
5	20	760.1	161.6	105	1159.8	269.5	125	0.0003 (***)
5	1000	845.2	232.9	100	1445.2	481.4	135	0.0015 (**)

Peak Calcium Concentration (Fig. 7):

K^+ (mM)	AT-II (pM)	WT mean (nM)	WT SD	WT (N)	Het mean (nM)	Het SD	Het (N)	P
3	0	1101.6	443.4	7	1386.2	654.9	10	Not tested
3	20	897.1	289.1	17	1263.9	135.5	6	0.0150 (*)
3	1000	941.5	206.4	90	1433.3	396.1	79	<0.0001 (***)
5	0	1206.8	254.6	3	1531.8	475.7	12	Not tested
5	20	1064.6	191.2	46	1505.1	332.5	28	0.0084 (**)
5	1000	1080.4	216.2	88	1702.8	542.9	111	0.0040 (**)

Activities (Fig. 7):

K^+ (mM)	AT-II (pM)	WT mean	WT SD	WT (N)	Het mean	Het SD	Het (N)	P
3	0	0.001	0.005	88	0.002	0.013	106	Not Tested
3	20	0.005	0.016	88	0.001	0.007	92	0.05709
3	1000	0.041	0.045	88	0.028	0.044	99	0.0442 (*)
5	0	0.000	0.002	79	0.002	0.011	117	Not Tested
5	20	0.018	0.035	79	0.015	0.039	117	0.9542
5	1000	0.146	0.095	79	0.100	0.087	128	0.0313 (*)

Activation Time Constants (Fig. S9):

K^+ (mM)	AT-II (pM)	WT mean (ms)	WT SD	WT (N)	Het mean (ms)	Het SD	Het (N)	P
3	1000	0.024	0.010	104	0.029	0.012	126	0.1235
5	1000	0.023	0.007	141	0.039	0.013	325	0.2373

Deactivation Time Constants (Fig. S9):

K^+ (mM)	AT-II (pM)	WT mean (ms)	WT SD	WT (N)	Het mean (ms)	Het SD	Het (N)	P
3	1000	0.810	0.378	102	0.609	0.160	126	0.3705
5	1000	0.813	0.406	141	0.771	0.359	323	0.9008

Intraburst Frequency (Fig. S10):

K^+ (mM)	AT-II (pM)	WT mean (Hz)	WT SD	WT (N)	Het mean (Hz)	Het SD	Het (N)	P
3	20	0.36	0.12	52	0.36	0.12	9	0.8695
3	1000	0.36	0.11	295	0.28	0.08	165	0.0026 (**)
5	20	0.35	0.09	101	0.31	0.08	170	0.0114 (*)
5	1000	0.34	0.09	756	0.29	0.08	773	0.0013 (**)

Burst Length (Fig. S10):

K^+ (mM)	AT-II (pM)	WT mean (s)	WT SD	WT (N)	Het mean (s)	Het SD	Het (N)	P
3	20	17.18	20.72	52	26.43	24.91	9	0.2245
3	1000	23.19	25.90	295	23.34	32.11	165	0.9562
5	20	29.84	39.45	101	25.27	37.93	170	0.3430
5	1000	33.70	50.07	756	27.99	43.09	773	0.0428 (*)

Number of Bursts (Fig. S10):

K^+ (mM)	AT-II (pM)	WT mean	WT SD	WT (N)	Het mean	Het SD	Het (N)	P
3	20	0.0011	0.0036	100	0.0001	0.0008	92	0.0414 (*)
3	1000	0.0066	0.0075	100	0.0033	0.0048	99	0.0152 (*)
5	20	0.0023	0.0045	98	0.0021	0.0059	117	0.8464
5	1000	0.0166	0.0115	98	0.0125	0.0114	128	0.0334 (*)

Movie S1 (separate file). Fura-2 recording (5 mM K^+) of a representative adrenal slice from a WT animal. Changes in Ang II concentration are indicated in the movie.

Movie S2 (separate file). Fura-2 recording (5 mM K^+) of a representative adrenal slice from a *Cacna1h*$^{M1560V/+}$ animal. Changes in Ang II concentration are indicated in the movie.

References

1. A. Nagy, M. Gertsenstein, K. Vintersten, R. Behringer, Manipulating the Mouse Embryo: A Laboratory Manual. Third Edition. *Cold Spring Harbor: Cold Spring Harbor Laboratory Press* (2003).
2. D. M. Bates, M.; Bolker, B.; Walker, S., Fitting Linear Mixed-Effects Models Using lme4. *Journal of Statistical Software* **67**, 1-48 (2015).
3. A. H. Zeileis, R., Diagnostic Checking in Regression Relationships. *R News* **2**, 7-10 (2002).
4. H. Wickham, *ggplot2: Elegant Graphics for Data Analysis* (Springer-Verlag, New York, 2016).
5. J. Schewe *et al.*, Elevated aldosterone and blood pressure in a mouse model of familial hyperaldosteronism with ClC-2 mutation. *Nat. Commun.* **10**, 5155 (2019).
6. G. Grynkiewicz, M. Poenie, R. Y. Tsien, A new generation of Ca2+ indicators with greatly improved fluorescence properties. *J. Biol. Chem.* **260**, 3440-3450 (1985).